Mon. Not. R. Astron. Soc. **348,** 469–481 (2004) doi:10.1111/j.1365-2966.2004.07308.x

On the origin of red giant depletion through low-velocity collisions

Tim Adams,[1]⋆ Melvyn B. Davies[1] and Alison Sills[2]

[1]*Department of Physics & Astronomy, University of Leicester, Leicester, LE1 7RH*
[2]*Department of Physics & Astronomy, McMaster University, 1280 Main St. W., Hamilton, ON, L8S 4M1, Canada*

Accepted 2003 October 15. Received 2003 October 11; in original form 2003 May 16

ABSTRACT

We investigate a means of explaining the apparent paucity of red giant stars within post-core-collapse globular clusters. We propose that collisions between the red giants and binary systems can lead to the destruction of some proportion of the red giant population, by either knocking out the core of the red giant or by forming a common envelope system which will lead to the dissipation of the red giant envelope. Treating the red giant as two point masses, one for the core and another for the envelope (with an appropriate force law to take account of the distribution of mass), and the components of the binary system also treated as point masses, we utilize a four-body code to calculate the time-scales on which the collisions will occur. We then perform a series of smooth particle hydrodynamics runs to examine the details of mass transfer within the system. In addition, we show that collisions between single stars and red giants lead to the formation of a common envelope system which will destroy the red giant star. We find that low-velocity collision between binary systems and red giants can lead to the destruction of up to 13 per cent of the red giant population. This could help to explain the colour gradients observed in PCC globular clusters. We also find that there is the possibility that binary systems formed through both sorts of collision could eventually come into contact perhaps producing a population of cataclysmic variables.

Key words: stellar dynamics – celestial mechanics – binaries: general – globular clusters: general.

1 INTRODUCTION

Observations of several post-core-collapse (PCC) globular clusters have revealed the existence of both population and colour gradients (Djorgovski et al. 1991). These observations have shown that the clusters become bluer towards the centre, and this is believed to be the result of a paucity of red giant stars and/or possibly an increase in the population of faint blue stars. The total effect represents a few per cent of the visible light.

Hubble Space Telescope observations (Bailyn 1994; Shara et al. 1998) have confirmed that there exists a depletion in the red giant population within several PCC clusters with respect to the horizontal branch. In addition, within several clusters, a population of supra-horizontal-branch (SHB) stars (stars which are much brighter than the normal horizontal branch and lie as a distinct population within an Hertzsprung–Russell diagram) have been identified. Shara et al. (1998) found a population of SHB stars in NGC6522 which were 1.5 mag brighter in the *B* band than the normal horizontal branch, whilst those found in 47 Tuc (Bailyn 1994) were a magnitude brighter than the local horizontal branch.

⋆E-mail: drtim_adams@hotmail.com

An additional interesting population of bright blue objects found in PCC are subdwarf B stars (sdB and related sdO/sdOB) (Sargent & Searle 1968). These are believed to be helium core burning objects with a small ($<0.02\ M_{\odot}$), but hydrogen-rich envelope. These stars cannot be formed through standard single main-sequence star evolution. Han et al. (2002) set out three methods for producing these stars through binary system evolution (through the ejection of a common envelope and the creation of a tight binary system, through Roche lobe overflow and through the merger of two helium white dwarfs). We propose the addition of a dynamical source for sdB stars where the core of an old, evolved, red giant is removed from the larger part of its envelope.

Within such a dense stellar system, it is inevitable that collisions between stars will occur. Indeed, collisions have been invoked as one possible mechanism for the creation of blue stragglers (see, for example, Fabian, Pringle & Rees 1975 or Sills et al. 2002), which are main-sequence stars with mass greater than the turnoff mass of the cluster in question. We now investigate the possibility that collisions between binary systems and red giants could explain not only the depletion of red giant stars but also the existence of some of the more exotic members of the stellar population. We also examine the outcomes of collisions between single bodies and red giant stars.

Previous work on collisions in globular clusters has focused on interactions between single bodies (be they main-sequence stars or degenerate bodies) and red giants. For instance, Davies, Benz & Hills (1991) examined collisions between a 0.8-$M_\odot$ red giant and impactors of mass 0.4 and 0.6 $M_\odot$ with velocities at infinity of 10 km s^{-1}. They found that for impact parameters less than twice the red giant radius, the impactor would become bound to the giant and some mass would be lost from the red giant envelope. Closer approaches would lead to more disruptive consequences for the red giant envelope. Rasio & Shapiro (1991) performed a similar set of simulations but found that any material which could go on to form a common envelope system was very quickly disrupted.

The work of Davies et al. (1998) looked at high-speed collisions between binary stars and red giants, collisions more pertinent to the galactic centre. They found that the most destructive encounters between binary systems and red giants were those which lead to either the knock-out of the red giant core, or those which ended up with a common envelope system. These two outcomes will be discussed in more detail in Section 3.

Beer & Davies (2003) have put forward an alternative suggestion to explain the paucity of red giants in PCC clusters. They argue that stars contained within binary systems could go through a double common envelope system as first one star reaches the red giant branch and then the other. During the common envelope stages, angular momentum would pass from the orbit of the binary system to the envelope gas, causing it to dissipate and causing the binary to harden. Indeed, it is possible that the two compact cores could actually merge in such a scenario.

We investigate interactions between binary systems and red giants in two complementary fashions. First, we examine the time-scales of relevance for the collisions utilizing an *N*-body technique. We then follow this up by utilizing detailed hydrodynamics to investigate the exact details of the collisions and to ensure that our *N*-body modelling technique is valid.

We also examine the outcomes of collisions between single bodies and red giants in an attempt to understand what impact these collisions can have on the population of red giants in a globular cluster.

In Section 2, we detail the observations which have motivated this work. In Section 3, we outline the theoretical considerations behind our model, before describing our numerical techniques in Section 4. In Section 5, we detail the results of our simulations of collisions between red giants and binary systems, before considering the subsequent evolution of the stars in Section 6. In Section 7, we look at other means of depleting the red giant population in low-velocity environments, such as single-star encounters. We discuss our conclusions in Section 8.

2 OBSERVATIONS

Observations over the past decade have identified the existence of a colour gradient within many globular cluster cores, in the sense of being bluer inward. Thus far, observations have only identified this phenomena within PCC clusters and not within those clusters fitted by the King model (KM).

Two distinct observation techniques have been used. These are not necessarily complementary and a colour gradient which shows up in one need not show up in the other. The first technique is direct surface photometry. Using such a technique, a colour gradient has been identified in, for example, M30 (Djorgovski et al. 1991). The second method is that of creating a colour pixel histogram (Bailyn et al. 1989). Two images of the clusters are taken in different bands (typically *U* and *B*) and the cleaned images are then divided. The resulting frame then maps the colour of the cluster rather than the intensity. A statistical analysis of the pixel colour distribution can then be utilized to compare different regions of the cluster. The first method is mainly sensitive to detecting the bright stars within the

Table 1. A table listing some of the globular clusters of our own galaxy, a description of their density profile (i.e. PCC or King model) and a description of any observed colour gradient.

Cluster	PCC or KM	Giant depletion?	Compared to what?	Colour gradient?	Extreme blue HB?	References
NGC 104 (47 Tuc)	KM	Y	AGB	N	N	Bailyn (1994), Auriere & Ortolani (1988), Cohen et al. (1997)
NGC 2808	KM	N	–	?	Y	Walker (1999)
NGC 4147	PCC?	N?	–	Y	Y	Djorgovski (1988)
NGC 5272 (M3)	KM	?	–	?	Y	Rosenberg et al. (2000)
NGC 5946	PCC	N	–	?	blue	Davidge (1995)
NGC 6093 (M80)	KM	?	–	N	Y	Djorgovski (1988)
NGC 6205 (M13)	KM	?	–	?	Y	Rosenberg et al. (2000)
NGC 6284	PCC	?	–	Y	Y	Djorgovski et al. (1991)
NGC 6293	PCC	Y	underlying light	Y	Y	Djorgovski et al. (1991)
NGC 6397	PCC	Y	underlying light	Y	Y,He WDs	Lauzeral et al. (1992), Djorgovski et al. (1991), Rosenberg et al. (2000)
NGC 6522	PCC	Y	HB	?	Y	Shara et al. (1998)
NGC 6558	PCC	?	–	Y	Y	Djorgovski et al. (1991)
NGC 6624	PCC	?	–	Y	N	Djorgovski et al. (1991), Rosenberg et al. (2000)
NGC 6626 (M26)	PCC	?	–	Y	Y?	Djorgovski (1988), Rosenberg et al.
NGC 6715 (M54)	KM	?	–	N	N	Djorgovski et al. (1991)
NGC 6864 (M75)	KM	?	–	N	Y	Djorgovski et al. (1991), Harris (1975)
NGC 7078 (M15)	PCC	Y	faint RGB, SG	Y	Y	Yanny et al. (1994), Djorgovski et al. (1991), Bailyn et al. (1989), Rosenberg et al. (2000)
NGC 7099 (M30)	PCC	Y	faint RGB, SG, underlying light	Y	N	Guhathakurta et al. (1998), Davidge (1995), Piotto, King & Djorgovski (1988), Burgarella & Buat (1996), Djorgovski et al. (1991)

cluster, whilst the second method is more adept at detecting the fainter population which cover the majority of the cluster.

In Table 1, we highlight some of the observations made of globular clusters within our own galaxy.

The two different methods typically result in different interpretations as to the cause of the colour gradient. The direct surface photometry normally suggests that there is an underabundance of luminous red giant stars (e.g. Djorgovski & Piotto 1993a), whilst the colour pixel histogram technique normally suggests an increased population of faint blue stars, including blue stragglers, towards the centre of the cluster (Bailyn et al. 1989). It is likely that the colour gradient in most clusters actually results from a combination of these two effects (Stetson 1994).

Given that colour gradients have only been confirmed within PCC clusters (3σ or more detection), it is suggestive that there could be some underlying dynamical explanations for their existence. Given the dynamical nature of core collapse, a collisional explanation for the depletion of red giants seems reasonable.

3 THEORY

3.1 Possible outcomes of red giant binary collisions

Globular clusters are crowded places. In particular, within PCC clusters the number densities of stars reach values in excess of 10^5 star pc^{-3}. Within such a dense environment, it becomes quite likely that collisions of some description will take place. Interactions involving binary systems are used to stave off core collapse (via binary heating) and direct collisions between stars have been proposed as a method of producing the blue straggler population seen within globular clusters.

In this paper, we are primarily interested in collisions involving binary systems and red giant stars (although, in Section 7, we do consider the outcomes of single-star collisions with red giants). Due to the contrast in size between the red giant and the components of the binary system (be they main-sequence stars or degenerate bodies) the binary components have been modelled as point masses in all simulations. In the four-body runs, the red giant has also been approximated as two point masses as well – one for the core and one representing the envelope. The details of this approximation are explained in Section 4.1.

During such an encounter, there are a number of distinct possible outcomes. These are detailed in Davies et al. (1998), and we shall only briefly mention the possible outcomes here.

(i) A *common-envelope* system may be formed where two of the point masses form a binary within the red giant envelope, whilst the third point mass is ejected.

(ii) A *knock-out* might occur where the core and envelope of the red giant become unbound. The binary system is also not bound to the envelope. This would completely destroy the giant.

(iii) All the bodies may become bound in a complex hierarchy. This is likely to be highly unstable and eventually reduce to one of the other outcomes.

(iv) A *fly-by* may occur where the binary simply passes by the red giant, leaving it relatively unperturbed.

(v) *Clean exchange*. This is a relatively unlikely event where the core of the red giant replaces one of the binary components. The ejected binary component then becomes the new core of the red giant.

(vi) *Ionization*. If the incoming binary is sufficiently soft, then it might be broken up by the encounter with the red giant. The two, now single, components could then remove some small quantity of mass from the red giant envelope.

(vii) *Ionization and exchange*. Again, the binary is broken up during the interaction; however, this time, one of the components replaces the red giant core at the centre of the envelope and the core escapes from the system.

Outcomes (i) and (ii) are effective means of destroying the red giant in a relatively short period of time. Outcome (iii) will also likely result in the destruction of the red giant as the bound system resolves into one of the other outcomes, primarily (i) and (ii). The subsequent evolution of outcomes (v) and (vii) is uncertain and will be dependent on exactly what the new 'core' is.

3.2 Common envelopes

During the collision, it is possible that some fraction of the red giant envelope gas will become bound to a binary system, formed of some combination of the members of the incoming binary system and the core of the giant. In this case, a common envelope system is likely to ensue. Within the common envelope system, angular momentum is removed from the orbit of the binary components, leading to the formation of a tighter binary (henceforth grinding down), and is passed to the envelope gas. This causes the ejection of the gas as it becomes unbound from the binary.

The details of common-envelope evolution are currently poorly understood. The best that we can do is to parametrize the situation in an attempt to understand what is going on. If we suppose that the binary is made up of the core of the red giant (of mass m_c)[1] and one of the interloping stars (of mass m_2), then with a red giant envelope of radius R_{env} and mass m_{env}, the binding energy of the envelope to the core is given by (de Kool 1990)

$$E_{bind} = \frac{G(m_c + m_{env})m_{env}}{\lambda R_{env}}, \tag{1}$$

where λ is a numerical factor describing the distribution of mass within the red giant. Our models yield values for λ between 0.3 and 0.5; however, this is for an undisturbed model and will change after a collision. As the binary is ground down within the envelope of material, its binding energy will change. This change is given by

$$\delta E_{orb} = \frac{Gm_2}{2}\left[\frac{m_c}{a_f} - \frac{m_c + m_{env}}{a_i}\right], \tag{2}$$

where a_i and a_f are the initial and final binary separations, respectively. If we assume that all this energy goes into unbinding the envelope with some characteristic efficiency α, then

$$E_{bind} = \alpha \delta E_{orb}, \tag{3}$$

whereupon a rearrangement for a_f gives

$$a_f = \frac{m_2 m_c}{2(m_c + m_{env})}\left[\frac{m_{env}}{\alpha\lambda R_{env}} + \frac{m_2}{2a_i}\right]^{-1}. \tag{4}$$

In Fig. 1, we plot the final separation of a binary against its initial separation (both in solar radii) for a range of α values. As can be seen in this plot, we can easily grind down a wide binary system to a tighter system. With less efficient α values, much tighter binary systems can be produced. This could provide a method of grinding down binaries and producing some of the interesting systems seen in globular clusters.

[1] In the case where the binary system is made up of the two components of the original binary, m_c is replaced with the mass of the component that the envelope is most bound to.

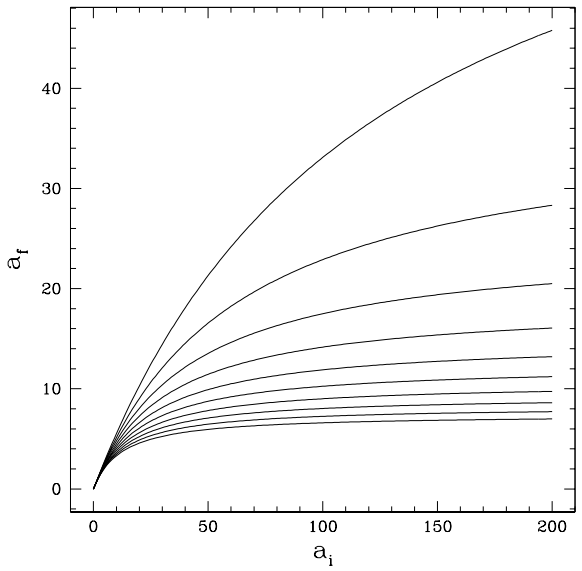

Figure 1. Final binary separation as a function of initial binary separation, both in solar units. We have plotted multiple curves for various α values. α decreases monotonically from 1 to 0.1 down the plot. This plot was produced for two equal-mass stars, $m_1 = m_2 = 0.8$ M$_\odot$, with $\lambda = 0.5$, $m_{\rm env} = 0.322$ and $R_{\rm env} = 100$ R$_\odot$.

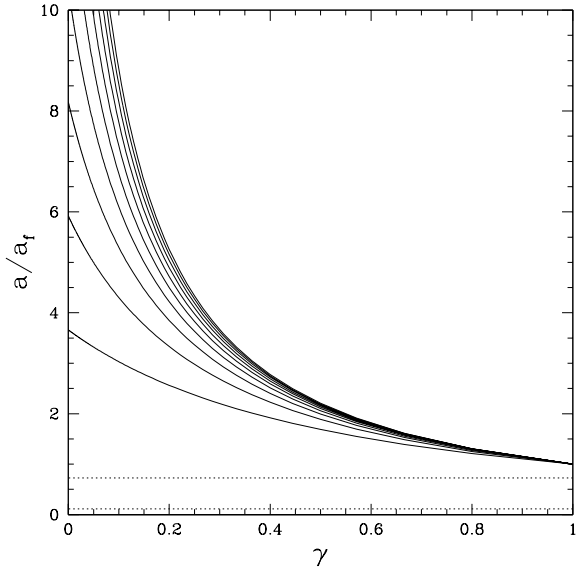

Figure 2. Ratio of the final separation of a binary system after undergoing a common envelope phase with some initial fraction, γ, of the total red giant envelope mass to the final separation if it were to have dispersed all the red giant envelope mass, taken as 0.322 M$_\odot$ as a function of γ. The multiple solid lines represent the effects of different α values, with α increasing monotonically from 0.1 to 1 from top to bottom. The dashed lines represent the ratio of the maximum size of the binary for a 0.8-M$_\odot$ main-sequence star to be just Roche lobe filling to the final separation of the binary if it were to have all the mass of the red giant envelope incommon envelope phase. As we can see, none of the binary systems quite come into contact through this common envelope phase. However, these calculations assumed an initially circular orbit; the introduction of some eccentricity would serve to bring the two components of the binary system closer to being Roche lobe filling. This plot was produced with $m_1 = m_2 = 0.8$ M$_\odot$, with $\lambda = 0.5$, $R_{\rm env} = 100$ R$_\odot$ and an initial binary separation of 100 R$_\odot$.

In Fig. 2, we plot the ratio of the final separation of a binary system which undergoes a common envelope phase with some initial fraction, γ, of the total envelope mass of the red giant to the final separation it would have had if $\gamma = 1$ as a function of γ. As can be seen, even a modest amount of mass is sufficient to cause a large reduction in the size of the binary orbit. Coupled to this is the effect of α. With less efficient α values, a tighter binary is formed for the same amount of envelope mass.

One might make a comparison between the time-scales associated with a binary collecting an envelope and hardening and the time required for scattering events to have the same effect. To do this, we first must identify the number of red giants within a cluster. Assuming that all stars within the mass range 0.8 to 0.81 M$_\odot$ (Beer & Davies 2003) are on the red giant branch, one can integrate a Salpeter-type mass function, $\mathrm{dN} \approx m^{-2.35}\,\mathrm{dM}$, to find $N_{\rm rg}$. Assuming that half of this population is contained within the central parsec of a globular cluster, an approximate time-scale for a binary to collide with a red giant is $\approx 3 \times 10^{15}$ yr. This is clearly a lower estimate, given our rather over optimistic assumption about the distribution of red giants. In reality, the time-scale is likely to be a lot longer. In contrast, the scattering time to get down to a separation of 10 R$_\odot$ from 100 R$_\odot$, assuming each scattering hardens the binary by 30 per cent, gives a time of $\approx 3 \times 10^{10}$ yr (assuming $v_\infty = 10$ km s^{-1}, $n = 10^5$ pc^{-3}). Clearly, it is far more likely that a binary will scatter down to a given separation, rather than collide with a red giant and pick up a common envelope.

One can compare the final separation of the binary after such a common envelope phase to that required for Roche-lobe overflow. Using the approximation of Eggleton (1983) for the size of the Roche lobe,

$$R_{\rm L} = \frac{0.49q^{2/3}}{0.6q^{2/3} + \ln(1+q^{1/3})}a, \tag{5}$$

where $q = m_2/m_1$, with m_2 being the mass of the secondary and m_1 is the mass of the primary, we can find the minimum separation required for a 0.8-M$_\odot$ star to be *just* Roche lobe filling whilst on the main sequence. We also assume that the primary has a mass of 0.8 M$_\odot$, which gives us an upper limit on the minimum separation. We plot two dashed lines in Fig. 2 representing the minimum size of the binary for Roche lobe overflow divided by the final separation of the binary if it had all the mass of the red giant envelope during the common envelope phase. The different lines represent the effects of different α values, with $\alpha = 0.1$ being the upper line and $\alpha = 1$ being the lower line. As we can see, it is not possible for this binary system to be ground down to a separation where Roche lobe overflow will take place whilst the star is still on the main sequence. For the binary to come into contact, we would require further angular momentum loss to occur. This could be through either gravitational radiation, which would occur on a time-scale of

$$\tau_{\rm gr} = 1.5 \times 10^8 \left(\frac{M_1}{\mathrm{M}_\odot}\right)^{-1} \left(\frac{M_2}{\mathrm{M}_\odot}\right)^{-1} \left(\frac{M_1+M_2}{\mathrm{M}_\odot}\right)^{-1} \times \left[\left(\frac{a_{\rm i}}{\mathrm{R}_\odot}\right)^4 - \left(\frac{a_{\rm f}}{\mathrm{R}_\odot}\right)^4\right] \mathrm{yr}; \tag{6}$$

assuming that the eccentricity of the system is negligible, although not necessarily true at the start of the evolution, the evolution of the binary toward a circular orbit is rapid. Alternatively, angular momentum may be lost through magnetic breaking on a time-scale of (Di Stefano & Rappaport 1992)

$$\tau_{\rm mb} = 4.3 \times 10^5 \left(\frac{M_1}{\rm M_\odot}\right) \left(\frac{\rm R_\odot}{R_2}\right)^{\zeta} \left(\frac{\rm M_\odot}{M_1 + M_2}\right)^2 \times \left[\left(\frac{a_{\rm i}}{\rm R_\odot}\right)^5 - \left(\frac{a_{\rm f}}{\rm R_\odot}\right)^5\right] {\rm yr}, \quad (7)$$

where R_2 is the radius of the main-sequence star. ζ is an adjustable parameter used to reflect the uncertainties in the physics behind the process of magnetic breaking; we assume $\zeta = 2$ (Davies 1997). If we look at the time-scales involved when all the bodies have a mass of 0.8 $\rm M_\odot$ (with one body being a main-sequence star and the other being a white dwarf) and an initial separation of 10 $\rm R_\odot$, the periods required to shrink the binary down to the point where the main-sequence star is just Roche lobe filling are $\tau_{\rm gr} = 1.4 \times 10^{12}$ yr and $\tau_{\rm mb} = 1 \times 10^{10}$ yr. Clearly, whether or not the binary will come into contact will be dependent on how much longer the star will stay on the main sequence, and the final dynamics of the binary system after the common envelope phase. What should be noted, however, is that these time-scales have been derived for a circular binary system. Clearly, in the case of a binary which has undergone some dynamical interaction, the binary will have some eccentricity and this could serve to dramatically lower the time-scales for bringing the binary into contact. Peters (1964) shows that for the gravitational radiation breaking mechanism, eccentricity can serve to reduce the merger time-scales of two bodies by a factor of 10^3 or more with sufficiently large eccentricities compared to a circular orbit. The effects of eccentricity on magnetic breaking and the effects during the common envelope phase are currently unknown, but it seems likely that they will reduce the in-spiral time as well. In any event, Roche lobe overflow will likely start as the star evolves off the main sequence and starts to expand.

With in-spiral times possibly as short as 10^9 yr, it is entirely possible that we could have a mechanism of producing a population of cataclysmic variables from binary systems that otherwise would not come into contact. These are binary systems containing a white dwarf accreting material from a low-mass main-sequence secondary star. Within the cores of globular clusters, it has been shown that any primordial population of cataclysmic variables (CVs) (i.e. a population of binary systems which will naturally evolve into a CV) will be severely depleted within the core due to collisions with other stars (Davies 1997). Thus having a method of producing a second generation of CVs is important to explain the population within the cores of globular clusters.

3.3 Knock-outs

To deplete the red giants from the cluster effectively, we need to remove the envelope of gas from around the core of the giant. Simply removing some proportion of the envelope gas will not be sufficient to prevent a star becoming a red giant as the expansion of the envelope is driven by the nuclear processes within the core of the star. Examination of our models has suggested that over 50 per cent of the envelope of the red giant would have to be removed before the evolution of the red giant was substantially altered. To knock the core out of a red giant star, it needs to receive sufficient energy to escape the potential well of the envelope material. In Table 2, we list the escape velocities of the two models used in this paper. These were calculated by integrating over the potential of the red giant envelope.

There are two sources of energy to free the core. The first is the incoming kinetic energy of the collision. In the case of a globular cluster, this is likely to be quite small ($v_\infty \approx 10\,{\rm km\,s^{-1}}$). The second source is through a hardening of the incoming binary system. When a binary system undergoes an interaction with a third star, it will either break up or get harder, depending on the initial binary separation (Heggie 1972). If the binary becomes harder during an interaction, potential energy is released and can be converted into kinetic energy.

Table 2. Details of the two 0.8-$\rm M_\odot$ red giant models we have used throughout this investigation. Escape velocities were calculated by integrating over the potential off the red giant envelope. The lifetime of a 0.8-$\rm M_\odot$ star on the red giant branch is approximately 8.7×10^7 yr. We have selected the two models which represent points near the middle and end of the branch.

Model	Time to the He flash (Gyr)	Core mass ($\rm M_\odot$)	Radius ($\rm R_\odot$)	Escape speed of core (km $\rm s^{-1}$)
A	0.05	0.284	11.672	249
B	≈ 0	0.478	111.01	53

We can simply equate the required kinetic energy for the core to escape from the envelope with a change in the binding energy of the binary system thus:

$$\frac{1}{2} m_{\rm c} v_{\rm esc}^2 = \beta E_{\rm bind}. \quad (8)$$

Using the data in Table 2, we see that we require the binary to get over 30 per cent harder for any initial binary separation over 60 $\rm R_\odot$. From the work of Heggie (1972), we know that, on average, interactions between binary systems and single stars result in only a 30 per cent hardening. This indicates that the ejection of the core through a simple hardening of the binary, whilst not impossible, is nonetheless likely to be a relatively rare event, given the wide population of binaries in globular clusters.

3.4 Collision probabilities

During the lifetime of a star, its radius changes markedly as a result of the nuclear processes going on within the core of the star. This variation in stellar radius is of crucial importance when one considers the collision cross-section, σ. Utilizing the Yale Rotating Evolution Code (YREC; Guenther et al. 1992), we calculated the radius of a 0.8-$\rm M_\odot$ star as a function of time. The collision cross-section, σ, is related to the stellar radius by

$$\sigma = \pi R_\star^2 \left[1 + \frac{2G(M_\star + M_{\rm int})}{R_\star v_\infty^2}\right], \quad (9)$$

where $M_{\rm int}$ is the mass of the interloping star.

In Fig. 3, we plot the integrated collision probability for a 0.8-$\rm M_\odot$ star as a function of its radius, which is indicative of its age, up to the helium flash. As we can see in this figure, the vast majority of collisions for the star are likely to occur during its main-sequence lifetime. However, we see that roughly 20 per cent of collisions will happen during the red giant phase of the life time of the stars. In particular, we note that 10 per cent of all collisions will occur when the radius of the red giant is between 10 and 100 $\rm R_\odot$, despite the fact that this actually represents a short period of time. For this reason, we have chosen to look at collisions involving red giants of these radii within this paper.

3.5 Red giant models

During our simulations, we have utilized realistic models of red giant stars produced using YREC. We have considered a single mass star, namely 0.8 $\rm M_\odot$ with a metallicity of [Fe/H] $= -1$, and have

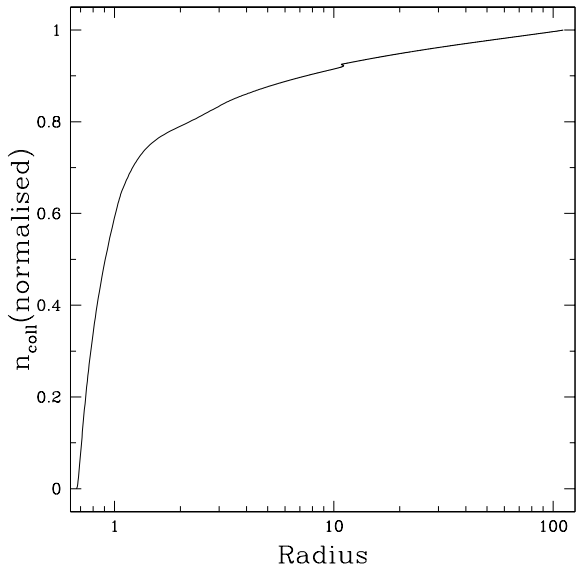

Figure 3. Integrated, normalized probability of a 0.8-$M_\odot$ star undergoing a collision as a function of its radius, which is a tracer of the age of the star. We have only considered the star up to the helium flash. As can be seen, the star will most likely undergo a collision during its main-sequence lifetime; this is due to the long main-sequence lifetime. Although the proportion of collisions occurring for the red giant during the period when its radius is between 10 and 100 $R_\odot$ appears to be low, it should be noted that the giant only spends of order 10^8 yr between these two radii. Thus this period represents the highest collision rate for the red giant.

considered it at two points through its evolution along the red giant branch (as detailed in the previous section). These points represent a point which is midway along the giant branch, at a time where the red giant has expanded to a radius of 11 $R_\odot$ and at the tip of the branch where the radius has reached a maximum size of 111 $R_\odot$. Although these points only sample a small proportion of the lifetime of post-main-sequence evolution of the star, they do represent the period where the red giant has a high collision rate.

4 NUMERICAL METHODS

We have taken two distinct paths in performing our simulations. To identify the time-scale associated with the collisions in a relatively quick fashion, we have utilized a four-body code (Davies et al. 1998). Then to check the reliability of our results and to examine the distribution of mass in the post-collision system, we have performed a number of hydrodynamical simulations.

4.1 4-body code

As mentioned in Section 3.1, we have modelled the interloping binary components, as well as the core of the red giants, as point masses. We also model the envelope of the red giant as a point mass with the proviso that we take into account that the force on any of the other point masses is dependent on the fraction, $f_{\rm enc}$, of envelope mass contained between the position of the point mass in question and the envelope centre. Thus, the force between the centre of the envelope, of total mass $M_{\rm env}$, and the ith point mass, a distance R apart, is given by;

$$\boldsymbol{F}_{i\rm env} = -G\frac{M_{\rm env}M_i f_{\rm enc}(R)}{|\boldsymbol{r}_i - \boldsymbol{r}_{\rm env}|^3}(\boldsymbol{r}_i - \boldsymbol{r}_{\rm env}). \tag{10}$$

For distances larger than the red giant radius, this force simply reverts back to being the force due to a point mass. With a functional form for $f_{\rm enc}(R)$ found for each of our red giant models, with R being the distance between the centre of the envelope and the ith point mass, we may write the equations of motion for the system as

$$\ddot{\boldsymbol{r}}_i = -G\sum_{j\neq i}\frac{M_j}{|\boldsymbol{r}_i - \boldsymbol{r}_j|^3}(\boldsymbol{r}_i - \boldsymbol{r}_j) - G\frac{M_{\rm env}f_{\rm enc}(R)}{|\boldsymbol{r}_i - \boldsymbol{r}_{\rm env}|^3}(\boldsymbol{r}_i - \boldsymbol{r}_{\rm env}), \tag{11}$$

$$\ddot{\boldsymbol{r}}_{\rm env} = -\frac{G}{M_{\rm env}}\sum_j\frac{M_{\rm env}f_{\rm enc}(R)M_j}{|\boldsymbol{r}_{\rm env} - \boldsymbol{r}_j|^3}(\boldsymbol{r}_{\rm env} - \boldsymbol{r}_j). \tag{12}$$

The force and potential resulting from the red giant envelope were tabulated and interpolation used to calculate forces and energies at particular separations.

Impact parameters for each collision were chosen at random from within the range 0 to $\rho_{\rm max}(v_\infty)$ as defined by Hut & Bahcall (1983):

$$\rho_{\rm max}(v_\infty) = \left(\frac{C}{v_\infty/v_{\rm c}} + D\right)a, \tag{13}$$

where C and D are numerical parameters (taken as 4 and 0.6, respectively) and a is the binary semimajor axis. The critical velocity, $v_{\rm c}$, is the velocity at w total energy of the system is zero:

$$v_{\rm c}^2 = G\frac{M_1M_2\left(M_1+M_2+M_{\rm rg}\right)}{M_{\rm rg}(M_1+M_2)}\frac{1}{a}. \tag{14}$$

For each individual collision within a run, we were able to classify the outcome as either one of those detailed in Section 3.1 or unclassifiable. We started by looking at the energy of the point masses relative to one another:

$$E_{ij} = -G\frac{M_iM_j}{|\boldsymbol{r}_i - \boldsymbol{r}_j|} + \frac{1}{2}\frac{M_iM_j}{M_i+M_j}(\dot{\boldsymbol{r}}_i - \dot{\boldsymbol{r}}_j)^2\begin{cases}\leqslant 0 \text{ bound}\\ \geqslant 0 \text{ unbound}\end{cases}, \tag{15}$$

with appropriate corrections applied if one of the point masses was within the red giant envelope. The closest binary system was first identified and then this was treated as a single point mass to see if the other point mass was bound to it; this process is iterated over the possible combinations of binary systems until the outcome of the collision is classified.

With the outcomes of the collisions classified, it is possible to calculate the cross-section of the particular interaction, by assuming it is some fraction of the total cross-section presented by the binary, thus:

$$\sigma_x = \pi\rho_{\rm max}^2(v_\infty)\frac{n_x}{n_{\rm tot}}, \tag{16}$$

where $n_x/n_{\rm tot}$ is the fraction of runs which produced the required outcome. Time-scales are then trivial to calculate via

$$\tau = \frac{1}{n\sigma_x v_\infty}. \tag{17}$$

For the purpose of our investigation, we assume a number density of binary systems, n, of 10^5 pc^{-3} and a velocity at infinity, v, of 10 km s^{-1}.

4.2 Hydrodynamical simulations

Utilizing a modified version of the Benz (1990) 3D smooth particle hydrodynamics (SPH) code, we performed a set of representative invasive encounters between the binary system and the red giants.

To the standard fluid particles, we introduced a number of point masses that interacted with both each other and the fluid particles solely through a gravitational force. The point masses were evolved on either their own unique time-step or on the smallest time-step of the SPH particles within the simulation (whichever was shortest) to ensure accuracy of the integration. Ee used the standard form of artificial viscosity, with $\alpha = 1$ and $\beta = 2.5$, and an adiabatic equation of state. The thermodynamic quantities are evolved by following the change in internal energy. Both the smoothing length and the number of neighbours can change in time and space. The smoothing length is varied to keep the number of neighbours approximately constant at $\sim$50.

For both of the models considered, the central concentration of the giants is sufficient that it becomes increasingly difficult to model them with a reasonable number of SPH particles. Instead, we have modelled the highly concentrated core of the giant with a point mass and then have this interact only via gravitational forces with a surrounding envelope of gas modelled with 50 000 SPH particles.

5 RESULTS

5.1 Determination of interaction time-scales

To gain an understanding of the time-scales involved in the binary–red giant interactions, a number of four-body simulations were performed. The red giant core and envelope were initially coincident and experienced an interaction with a binary system as described in Table 3.

200 collisions were simulated for each of the runs described in Table 3. For each run, the phase and orientation of the binary with respect to the red giant are random. In Fig. 4, we plot the time-scales for knock-out events (crosses), common envelope formation (filled triangles) and all-bound systems (filled squares). In addition, we also plot the time-scale for a more general destructive collision to occur (i.e. any of the prior three outcomes) as a filled circle. As can be seen in the figure, there is a trend of decreasing time-scale with increasing red giant radii, as one would expect. In addition we also see a trend of decreasing time-scale with increasing mass of the binary component. Again, this is as expected due to the gravitational focusing term in the cross-section equation. On the figure, we plot

Table 3. A list of the four-body runs performed to examine the phase space of the collisions. For each of the runs detailed above, 200 simulations of collisions between the red giant and the binary system were performed using a randomly selected set of incoming parameters. M_1 and M_2 are the masses of the binary components, whilst M_3 is the mass of the red giant core and M_4 is the mass of the red giant envelope.

RunID	M_1	M_2	M_3	M_4	a R$_\odot$ ($R_{\rm rg}$)	$R_{\rm rg}$
1	0.8	0.8	0.27	0.53	5.5 (0.5)	11.0
2	0.8	0.8	0.27	0.53	11.0 (1.0)	11.0
3	0.8	0.8	0.27	0.53	22.0 (2.0)	11.0
4	0.8	0.8	0.49	0.31	56.0 (0.5)	111.0
5	0.8	0.8	0.49	0.31	111.0 (1.0)	111.0
6	0.8	0.8	0.49	0.31	222.0 (2.0)	111.0
7	1.4	0.8	0.27	0.53	5.5 (0.5)	11.0
8	1.4	0.8	0.27	0.53	11.0 (1.0)	11.0
9	1.4	0.8	0.27	0.53	22.0 (2.0)	11.0
10	1.4	0.8	0.49	0.31	56.0 (0.5)	111.0
11	1.4	0.8	0.49	0.31	111.0 (1.0)	111.0
12	1.4	0.8	0.49	0.31	222.0 (2.0)	111.0

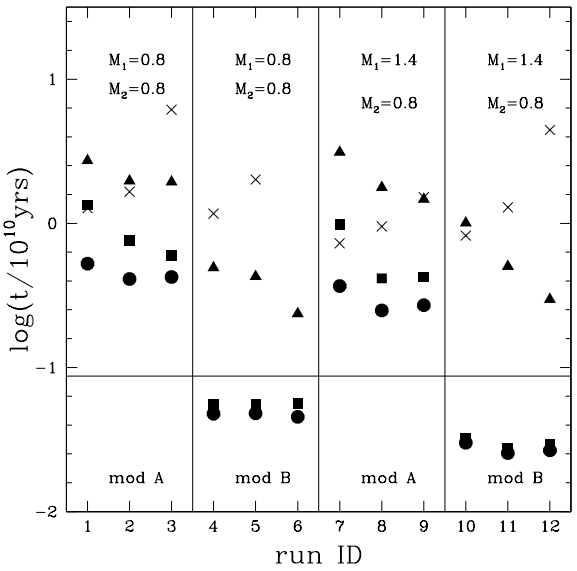

Figure 4. Plot of the various time-scales for events to occur in a cluster with a binary number density of 10^5 pc^{-3} and for a velocity at infinity of 10 km s^{-1}. The run IDs are as in Table 3. Crosses represent knock-out events, filled squares represent all-bound events and the filled triangles represent common-envelope events. The filled circles represent the *interesting* time-scale, i.e. that on which one of the destructive events will happen to the red giants.

a horizontal line representing the lifetime of a 0.8-M$_\odot$ star on the red giant branch. As can be seen, this lies below all the other time-scales except for the larger giant. This indicates that interactions between binary systems and red giants will at most be responsible for depleting only a few per cent of the red giant population.

We see that events which result in all objects being bound have the lowest time-scales, particularly for the older red giant star (model B). Clearly, this makes sense, as the older the red giant, the larger the cross-section it presents and the less bound the core is to the envelope.

However, one must recall that the time that the red giant spends between these two radii is very short compared to the lifetime of the giant. Indeed, the period is only of order 5×10^7 yr, less than a tenth of the life of the red giant. Thus from these results, it seems unlikely that collisions between red giants and binary stars could be responsible for explaining the destruction of all the missing red giants.

5.2 Detailed hydrodynamics

We performed a number of SPH simulations which were representative of those performed within the four-body runs to ensure that the point mass approach was accurate (all of these simulations were performed in the orbital plane of the binary system); these are detailed in Table 4. The most striking feature which came out of these simulations was the propensity for the smaller separation binary system to become bound to the red giant star once one of the stars of the binary started passing through the envelope of the red giant – slightly more so than had been predicted by the four-body simulations. This is not entirely unexpected. The work of Davies et al. (1991) centred on collisions between single stars and red giants. They found that once an interloping star came within 2 $R_{\rm rg}$, tides could be raised and energy dissipated, resulting in a bound system with an eccentric orbit. If the star came within 1.6 $R_{\rm rg}$, it would eventually spiral

Table 4. Details of the representative SPH simulations that we performed. We used a model B star made up of 50 000 SPH particles with a point mass at its core, as described in Section 4.2. The minimum distance refers to the distance between the centre of mass of the binary system and the core of the red giant.

Run	$a/\mathrm{R}_\odot$	$R_{\min}/\mathrm{R}_\odot$	M_1	M_2
1	22	0	0.8	0.8
2	22	21	0.8	0.8
3	22	40	0.8	0.8
4	22	80	0.8	0.8
5	56	29	0.8	0.8
6	56	38	0.8	0.8
7	56	80	0.8	0.8
8	56	120	0.8	0.8
9	111	0	0.8	0.8
10	111	61	0.8	0.8
11	111	66	0.8	0.8
12	111	81	0.8	0.8
13	111	120	0.8	0.8
14	222	112	0.8	0.8
15	222	117	0.8	0.8
16	222	137	0.8	0.8
17	222	190	0.8	0.8

into the red giant envelope on subsequent periastron passages. Thus in our simulations it is clear that most invasive collisions will result in an all-bound system, which will evolve to one of the other possible outcomes after some period of time. The exact outcome of the unstable triple is impossible to predict. However, we can make tentative predictions based on previous numerical simulations. It is likely that interactions within the system will eventually result in a kick being given to the lightest member of the hierarchy, which then escapes, carrying away whatever mass is bound to it.

In Fig. 5, we plot the mass retained by the core and the mass of the envelope gas which is no longer bound to the system as a function of the ratio of binary semimajor axis to minimum distance of approach (where the minimum distance of approach is measured relative to the centre of mass of the binary system). As can be seen, there is an anticorrelation between the two quantities, as one might expect. For collisions during which the binary system moves deep into the red giant envelope, the chances of a close encounter between one of the binary components and the core is increased. Such an encounter would lead to a much increased velocity for the core, which would rapidly move out of the envelope. This then means that less mass can be bound to the core, thus explaining the increased mass loss from the envelope.

In Fig. 6, we plot the mass of envelope gas which has become gravitationally bound to the binary system in a common envelope system, as a function of the ratio of the binary separation and minimum distance of approach. As can be seen, there is no discernible pattern within this plot, but what we do see is that it is possible for the binary to pick up a non-negligible envelope of material. This material could be important for grinding down the binary, as we have discussed.

In Fig. 7, we show a time-series plot of one of our SPH simulations. As can be seen, the point masses of the binary system have surrounding envelopes of gas particles, whilst the core of the red giant is relatively isolated in comparison.

As mentioned earlier, from the SPH simulations, we found that the formation of an all-bound system (i.e. one where all of the point

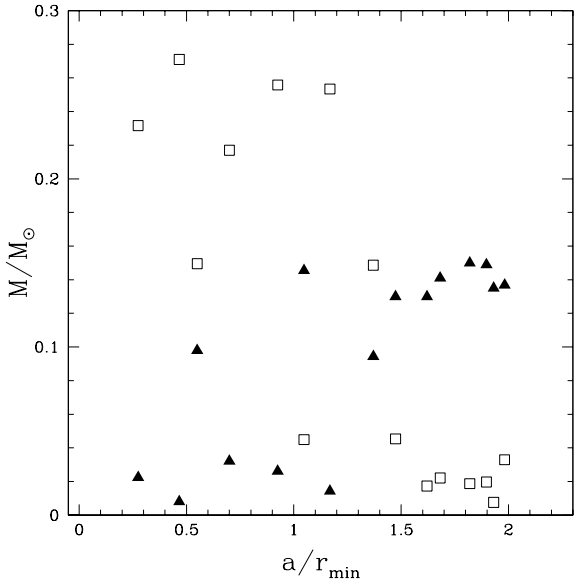

Figure 5. A combined plot of the mass still bound to the core of the red giant as a function of the ratio of the binary separation and minimum distance at approach (denoted as opened squares), and the total mass no longer bound to any of the point masses or binary systems (filled triangles). As can be seen in the plot, for deeper, more invasive collisions, more mass is lost from the system; at the same time, less mass remains bound to the core. For less invasive collisions, the opposite is true: more mass remains bound to the core of the red giant, whilst only a small amount of mass is no longer bound to the system. Initially, the total mass of the envelope was 0.322 $\mathrm{M}_\odot$.

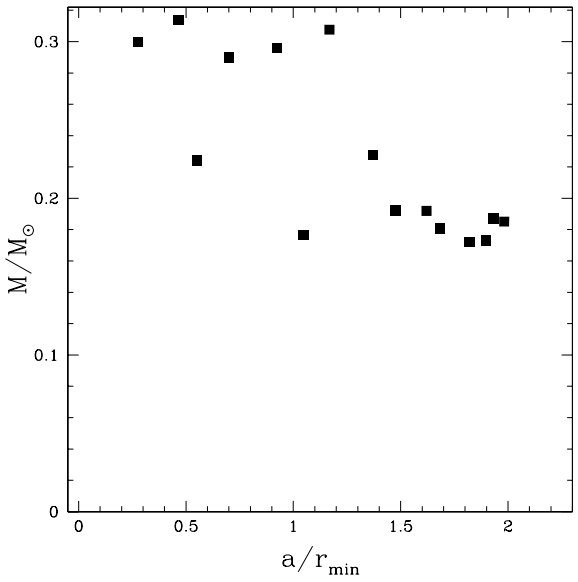

Figure 6. Common envelope mass as a function of the ratio of binary separation to the minimum distance of approach. As can be seen, there is no clear discernible pattern within the figure. The subsequent evolution of the all-bound system is likely to add to the mass of gas in the common envelope as close approaches of the three point masses will serve to disrupt their individual gaseous envelopes.

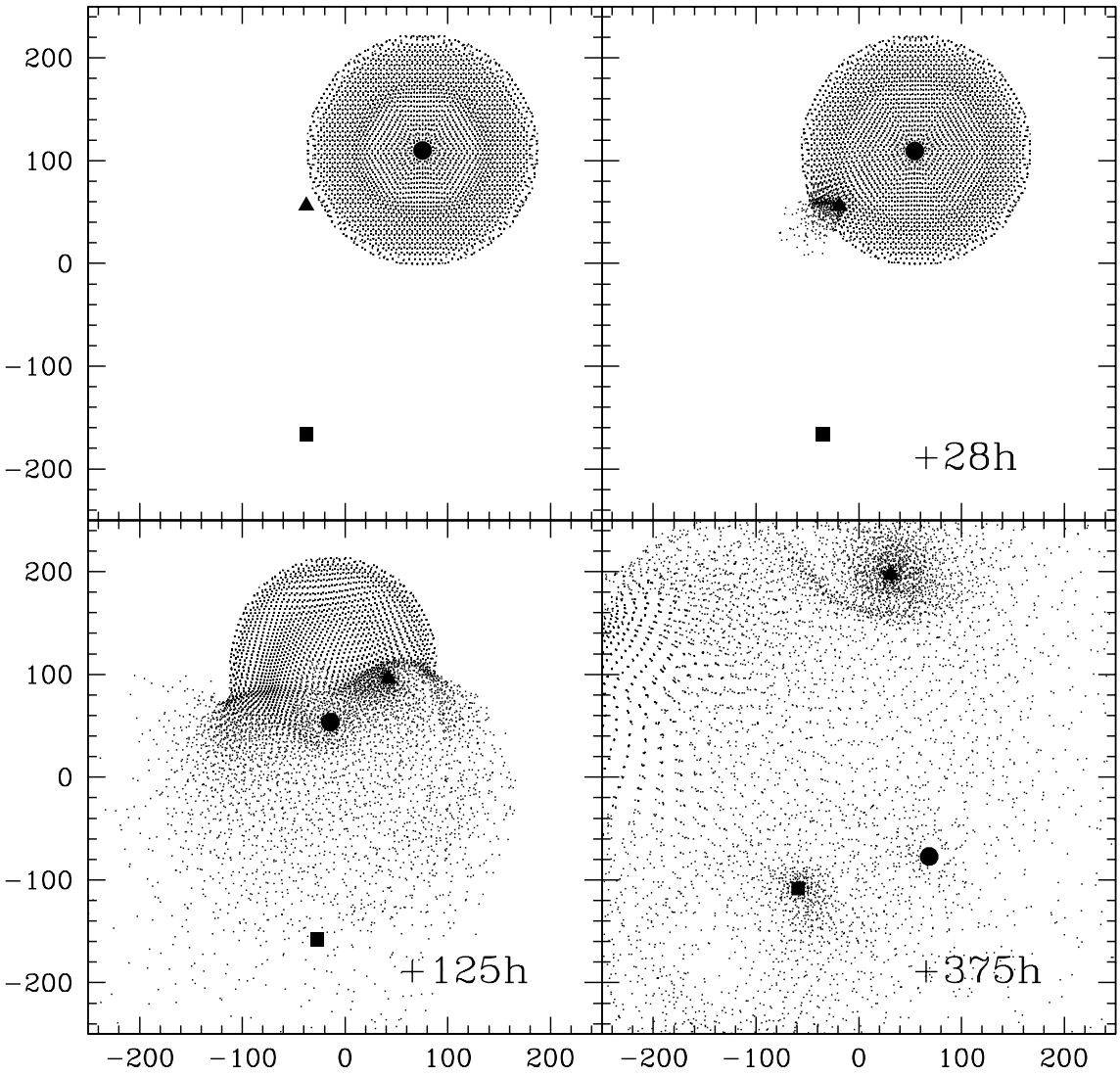

Figure 7. Time-series particle plot of a collision between a model B red giant and a binary system of separation 222 $R_\odot$ with a minimum distance of approach between the core of the red giant and the centre of mass of the binary system of 137 $R_\odot$. The core of the giant is represented by the circle, whilst the square and the triangle represent the components of the binary system. The figure shows only those particles within 2 h of the $z = 0$ plane. All three of the heaviest bodies, the core and binary system components, are bound in the final snapshot. The system will continue to evolve until eventually one of the three bodies is ejected – most probably the light core. The time from the first panel (in h) is indicated in each of the panels.

masses are bound together) was somewhat increased for the collisions involving the smaller separation binary systems compared with the predictions of the four-body code. There was no increase for the larger systems. We attribute this to the dissipation of the incoming kinetic energy through shocks which can be modelled within the SPH but not in the *N*-body approach. For the larger separation binary systems, the potential energy between the core and one of the components is higher than the potential between the two components of the binary system, even when the binary just grazes across the surface of the red giant. Thus it is likely that an all-bound system will result from the collision. In the case of the smaller systems, this is not the case. Instead, we need to dissipate more of the kinetic energy of the collision for the core to become bound to the binary system. To calculate more accurate cross-sections for the destructive encounters between the smaller separation binary systems and the red giants, we re-examined the collisions performed with the four-body code and selected out all those in which one member of the binary system came within 75 per cent of the red giant radius of the core. These collisions will almost certainly lead to the formation of an all-bound system and the subsequent destruction of the red giant. We assumed a binary population number density of 10^5 pc^{-3} and velocity dispersions of 10 km s^{-1}. We found that up to 13 per cent of the red giant population could be destroyed through collisions with binary systems independent of the binary separation.

One can make a prediction of what proportion of the red giant population we would expect to destroy through collisions using the encounter time-scale of Binney & Tremaine (1987):

$$\tau_{\rm enc} = 7 \times 10^{10} \frac{n}{10^5/{\rm pc}^3} \frac{{\rm M}_\odot}{M_{\rm tot}} \frac{{\rm R}_\odot}{r_{\rm min}} \frac{v_\infty}{10\ {\rm km\ s}^{-1}}\ {\rm yr}. \quad (18)$$

If we again assume a number density, n, of 10^5 pc^{-3} along with a $v_\infty = 10$ km s^{-1} and a total mass of 2.4 $M_\odot$ (i.e. the masses of

the binary components are the same as the mass of the red giant), then for an encounter within 100 $R_\odot$, we find $\tau_{enc} = 2.9 \times 10^8$ yr. Comparing this to the period that the red giant spends with a radius of approximately 100 $R_\odot$, we find that around 17 per cent of the red giant population will undergo a collision.

6 SUBSEQUENT EVOLUTION

During the majority of the SPH-performed collisions, we saw the formation of a complex triple system where the two components of the initial binary system and the core of the red giant were bound in some complicated arrangement. Such a system is highly unstable and, through further interactions, one of the binary systems will harden and the other body will be ejected from the system. It is highly likely that the ejectee will be the core of the red giant as it has a lower mass than either of the initial binary components. During the collision, the envelope of the giant is stirred up and forced to expand as energy is dumped into it. As this occurs, the binding energy of the core of the red giant to the envelope is reduced; as a consequence, the escape velocity of the core is much lower than in the pre-collision state. The expanded state of the envelope means that it is unlikely that the escaping core will pick up any significant additional material as it passes through it.

The subsequent evolution of the isolated core will be dependent on its mass and the mass of its now small envelope. Cores which are removed from the largest giants are about to start helium burning, so it is entirely possible that these cores could form the population of subdwarf B stars we discussed in the introduction if they carry away sufficient mass in their envelopes ($<0.05\ M_\odot$). Cores from younger giants (i.e. those which have just moved on to the subgiant branch) with a non-negligible envelope (40 per cent or more of the original envelope) will likely follow a stunted evolutionary path similar to that of a normal giant. There will be obvious differences in the exact evolution, but possibly these stars can go on to populate the normal horizontal branch, thereby removing any problem with numbers in the two branches.

The binary system which remains will be surrounded by at least a cursory common envelope system. Dynamical friction between the components of the binary and the gas in the envelope will transfer angular momentum away from the binary system, leading to its shrinkage and the expulsion of the gas. The degree to which the binary shrinks is highly dependent on the mass of the envelope and the efficiency factor α. It is entirely possible that the binary could shrink down to the point where the components come into contact, as described in Section 3.2. This could be useful in explaining some of the more exotic binary systems found within globular clusters. The mass of the envelope may well be increased as the system evolves. It is possible that periastron passages within the triple system may be close enough to disrupt the disc of material surrounding each of the individual bodies, moving mass out of the discs into the common envelope.

As discussed in Section 3.2, the end of the common envelope phase is not the end of the evolution for the binary system. It will continue to harden through gravitational radiation and magnetic breaking. The binaries formed during these interactions are all quite eccentric. If they retain some proportion of this eccentricity past the common envelope phase, then the in-spiral time of the binary can be dramatically reduced (Peters 1964). Thus if one of the components of the binary system is a main-sequence star of sufficiently low mass and the other body is a white dwarf, then it is entirely possible that the binary could be ground down to the point where the main-sequence star is filling its Roche lobe and thus producing a cataclysmic variable.

Table 5. Details of the collisions between a red giant and a single body. The minimum distance of approach in these runs is the same as those in the runs performed in Rasio & Shapiro (1991). We have used our model B red giant.

Run	r_{min}/R_{rg}	v_∞ 10 km s^{-1}
1	0.05	10
2	0.20	10
3	0.5	10
4	1.0	10
5	2.0	10
6	2.5	10

7 OTHER METHODS OF DEPLETING GIANTS

Our simulations have shown that whilst collisions between binary stars and red giants can effectively destroy a red giant, the timescales involved suggest that there would have to be an additional depletion method. One possibility is that proposed by Beer & Davies (2003), where the red giant is contained in a binary system and a double common envelope system could occur, effectively destroying the red giant.

Another possible explanation for the paucity of red giants is that collisions with other single stars could lead to their destruction. Rasio & Shapiro (1990) claim through a series of *N*-body simulations that the envelope of the giant is almost immediately dissipated during such a collision and a binary system is formed. In Rasio & Shapiro (1991), a series of SPH simulations were performed. Instead of dissipating the red giant envelope, they find that material goes into forming a large disc around the impacting star. Davies et al. (1991) performed SPH simulations of similar collisions and found that whilst the impactor and the core would become bound,

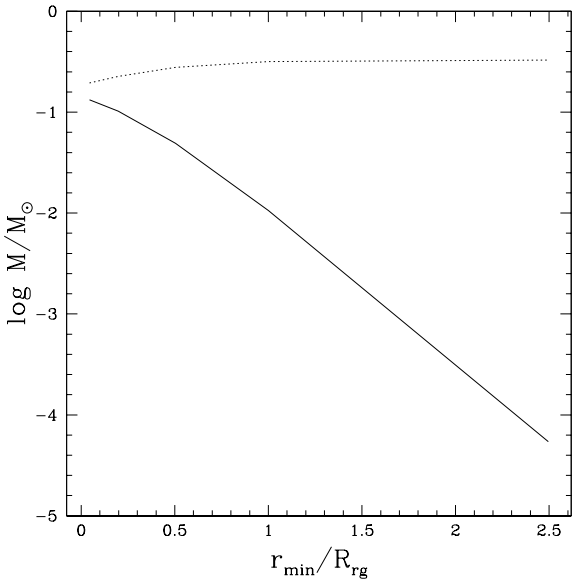

Figure 8. Mass retained (dashed line) and mass lost (solid line) from the red giant envelope as a function of the minimum separation between the red giant core and the impactor. This plot is produced after the initial impact. As can be seen, deeper impacts result in far more mass loss from the system. We have summed all the mass still bound to the system, as Fig. 10 shows that the system undergoes further mass loss during subsequent periastron passages.

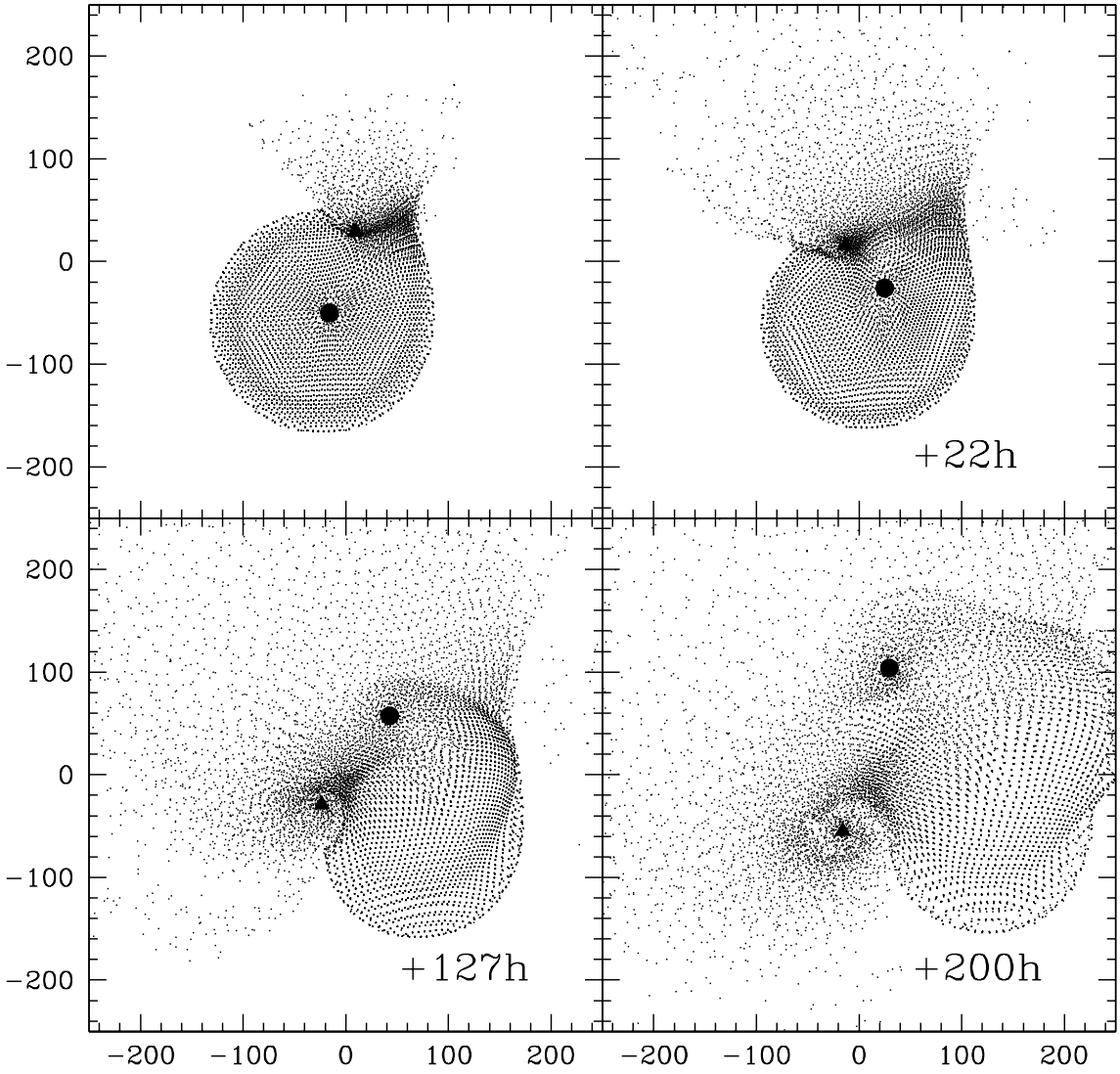

Figure 9. A collision between a red giant star and a single body. As can be seen, initially a disc is formed around the interloping star; however, the core and the interloping star are bound on orbits which bring them back together with a periastron separation which is small enough for the disc of material to be disrupted and the mass redistributed into the common envelope.The time from the first panel (in h) is indicated in each of the panels.

the immediate ejection of the envelope did not occur. Instead, a common envelope phase would start; as a result, the binary would spiral in and the envelope would be dissipated. In an effort to determine which of these two arguments are correct, we performed the collisions detailed in Rasio & Shapiro (1991) utilizing our SPH code and models. The details of the collisions performed are in Table 5.

In all the collisions, we found that sufficient energy could be dissipated so that the core and the interloping star became bound in eccentric orbits which had periastron passages smaller than the initial distance of closest approach. In the deeply invasive collisions, we found that *initially* a large disc (more accurately, a flattened spheroid) of material would form around the interloping star, whilst the core retained very little gas mass. However, the disc was sufficiently large that during periastron passages the core would pass through it and the disc would be broken up (later in this section, we shall discuss this further). For less invasive collisions, the core of the red giant would retain most of the mass, but again, subsequent periastron passages would result in this material being disturbed. In Fig. 8 we show how much mass was lost from the system and how much remains bound to it as a function of the minimum distance of approach. As can be seen, the mass loss is very sensitive to the minimum distance of approach, with very little mass lost for more grazing collisions. In Fig. 9, we show a time-series plot of the particles laying within 2 h of the $z = 0$ surface for one of the collisions. We can see that initially there is a disc formed around the impacting star. In Fig. 10, we show the evolution of the separation of the two point masses for the collision shown in Fig. 9, along with the mass loss from the system as a function of time.

In the upper panel of Fig. 10, we show the evolution of the separation of the binary components for one of the simulations ($R_{\rm min} = 0.5R_{\rm rg}$). As can be seen, the core and the impactor are initially on large eccentric orbits; however, the periastron separation is sufficiently small that the bodies pass within the disc of material around each other. This results in further dissipation of energy and the orbit of the two bodies is shortened. In addition, the mass within the system is again redistributed; some goes into the common envelope, whilst some escapes, as shown in the lower panel of Fig. 10. After a sufficient number of periastron passages, the disc

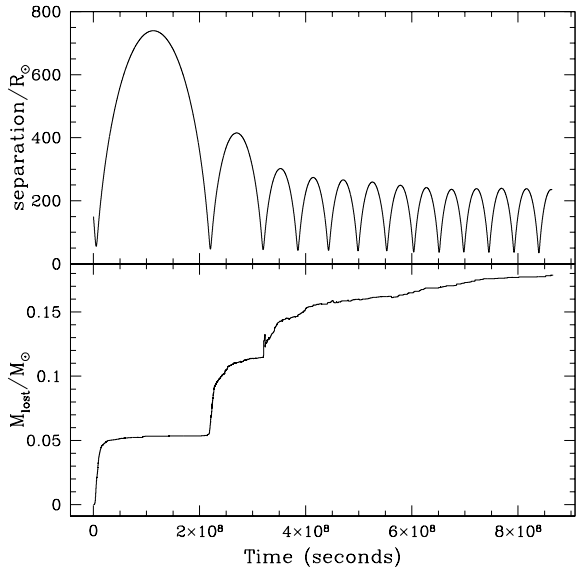

Figure 10. In the upper panel, we show the evolution of the separation between the two components of a binary system formed after a collision between a red giant and an impactor with a minimum distance of approach of $0.5\,R_{\rm rg}$. As can be seen, each periastron passage results in the dissipation of energy and a subsequent decrease in the binary separation. In the lower panel, we plot the total mass lost from the system. As can be seen, each time there is a periastron passage, we get a wave of mass loss as the discs of material around the two objects are disrupted. This simulation was performed with 5000 particles. A comparison between the escaping mass fraction for this simulation was made with the initial portions of a 50 000 particle simulation; there were no significant differences.

of material is completely broken up and the mass loss rate from the system is substantially reduced. At this point, all the bound material is smothering the binary system in a common-envelope-type scenario. Within this common envelope, the binary will further harden, as detailed in Section 3.2. As with the binary systems produced in Section 5.2, after the common envelope phase, the binary will continue to evolve through the mechanisms described in Section 3.2, and these systems may also go on to form a population of cataclysmic variables, although with a smaller white dwarf mass. This is more in agreement with the results of Davies et al. (1991), although the early stages of the binary evolution are similar to those presented by Rasio & Shapiro (1991). We simply allow the system to evolve for longer.

In higher-velocity regimes, such as the galactic centre, single-star collisions are less likely to result in the formation of a common envelope. This is because it is impossible to dissipate sufficient kinetic energy in the red giant envelope to allow the core and interloping star to become bound. Instead, these collisions are more immediately destructive and close encounters between the core and the interloping stars will result in the core being ejected with only a very small amount of gas. A larger minimum distance of approach will result in large amounts of the envelope gas becoming unbound due to the input of kinetic energy from the interloping star.

8 CONCLUSIONS

We have shown that collisions between binary systems and red giant stars could be responsible for depleting up to 13 per cent of the red giant population in dense globular clusters. The passage of one of the components of the binary system through the envelope results in sufficient dissipation of energy that the binary system and the red giant become bound. The subsequent evolution of this triple system is likely to be destructive to the red giant and provides an effective method of removing the giant. During the collision, an envelope of material becomes bound to the binary system. This will lead to the binary spiralling inwards as angular momentum is passed from the orbit of the two stars to the envelope gas. This could play a role in producing some of the very close binary systems, although it should be noted that the time-scale for an individual binary to pick up an envelope of gas from a red giant and then shrink through a common envelope phase is much longer than the time required for the same binary to undergo multiple scattering events and harden down to the same separation. These close systems may go on to further harden through angular momentum losses in the form of gravitational radiation or magnetic breaking and eventually come into contact, thus producing a population of cataclysmic variables.

Djorgovski & Piotto (1993a) present evidence suggesting that red giants may be depleted by up to 50 per cent in some clusters. Clearly, our dynamical method of destroying giants cannot be responsible for all of the observed depletion. Instead, it must work alongside other methods, such as that proposed by Beer & Davies (2003).

There are important differences between this and previous work. In Davies et al. (1998), collisions between red giants and binary systems in the galactic centre were considered. There it was found that bound systems were seldom formed. This difference can easily be attributed to the difference in the relative velocities between our work and theirs. Collisions in the galactic centre have a much higher velocity at infinity, and during a collision with a red giant, it is not possible to dissipate sufficient kinetic energy for the interloper to become bound to the red giant.

In addition, we have also looked at low-velocity collisions between red giant stars and single stars. We have shown that, on the initial impact, a large disc of material can form around the impactor if the minimum distance of approach is sufficiently small. However, the core and the impactor are on a bound orbit and subsequent periastron passages are sufficiently close that any material which is in a disc around one of the bodies is disrupted.

In conclusion, we can say that any physical collision is detrimental for the life expectancy of a red giant. The low-velocity dispersion within a globular cluster means that a bound system is a virtual certainty, and the ensuing common envelope phase or disruption of the red giant envelope with each periastron passage will quickly remove the red giant from the cluster.

ACKNOWLEDGMENTS

TAD gratefully acknowledges a PPARC studentship. MBD gratefully acknowledges the support of a URF provided by the Royal Society. AIS is funded through NSERC. Theoretical astrophysics at Leicester is supported by a PPARC rolling grant. The computations reported here were performed using the UK Astrophysical Fluids Facility (UKAFF), the University of Leicester Mathematical Modelling supercomputer funded through EPSRC, and the cluster facility at Leicester supported by AMD, Crucial and 3-Com. We would also like to thank the referee whose comments helped improve this paper.

REFERENCES

Auriere M., Ortolani S., 1988, A&A, 204, 106
Bailey V. C., Davies M. B., 1999, MNRAS, 308, 257
Bailyn C., 1994, AJ, 107, 1073
Bailyn C. D., Grindlay J. E., Cohn H., Lugger P. M., Stetson P. B., Hesser J. E., 1989, AJ, 98, 882
Beer M. E., Davies M. B., 2003, MNRAS, submitted
Benz W., 1990, in Buchler J. R., ed., The Numerical Modelling of Nonlinear Stellar Pulsations: Problems and Prospects. Kluwer, Dordrecht, p. 269
Binney J., Tremaine S., 1987, Galactic Dynamics. Princeton Univ. Press Princeton, NJ
Burgarella D., Buat V., 1996, A&A, 313, 129
Cohen R. L., Guhathakurta P., Yanny B., Schneider D. P., Bahcall J. N., 1997, AJ, 113, 669
Davidge T. J., 1995, AJ, 110, 1177
Davies M. B., 1997, MNRAS, 288, 117
Davies M. B., Benz W., Hills J.G., 1991, ApJ, 381, 449
Davies M. B., Blackwell R., Bailey V. C., Sigurdsson S., 1998, MNRAS, 301, 745
De Kool M., 1990, ApJ, 358, 189
Di Stefano R., Rappaport S. A., 1992, ApJ, 396, 587
Djorgovski S., 1988, in Grindlay J., Phillip A. G. D., eds, Proc. IAU Symp. 126, Globular cluster systems in galaxies. Reidel, Dordrecht, p. 333
Djorgovski S., Piotto G., 1993a, in Djorgovski S. G., Meylan P. G., eds, ASP Conf. Ser. Vol. 48, Structure and Dynamics of Globular Clusters. Astron. Soc. Pac., San Francisco, p. 203
Djorgovski S., Piotto G., 1993b, in Smith G. H., Brodie J. P., eds, ASP Conf. Ser. Vol. 50, The Globular Clusters–Galaxy Connection. Astron. Soc. Pac., San Francisco, p. 84
Djorgovski S., Piotto G., Phinney E. S., Chernoff D. F., 1991, ApJ, 372, L41
Eggleton P. P., 1983, ApJ, 369, 368
Fabian A. C., Pringle J. E., Rees M. J., 1975, MNRAS, 172, 15
Guenther D. B., Demarque P., Pinsonneault M. H., Kim Y.-C., 1992, ApJ, 392, 328
Guhathakurta P., Webster Z. T., Yanny B., Schneider D. P., Bahcall J. N., 1998, AJ, 116, 1757
Han Z., Podsiadlowski Ph., Maxted P. F. L., Marsh T., Ivanova N., 2002, MNRAS, 336, 449
Harris W. E., 1975, ApJS, 29, 397
Heggie D. C., 1972, in Lecar M., ed., The Gravitational, *N*-body Problem. Reidel, Dordrecht, p. 148
Hut P., Bahcall J. N., 1983, ApJ, 268, 319
Lauzeral C., Ortolani S., Auriere M., Melnick J., 1992, A&A, 262, 63
Peters P. C., 1964, Phys. Rev., 136, 1224
Piotto G., King I. R., Djorgovski S., 1988, AJ, 96, 1918
Rasio F. A., Shapiro S. L., 1990, ApJ, 354, 201
Rasio F. A., Shapiro S. L., 1991, ApJ, 377, 559
Rosenberg A., Aparicio A., Saviane I., Piotto G., 2000, A&AS, 145, 451
Sargent W. L. W., Searle L., 1968, ApJ, 152, 443
Shara M. M., Drissen L., Rich R. M., Paresce F., King I. R., Meylan G., 1998, ApJ, 495, 796
Sills A., Adams T., Davies M. B., Bate M. R., MNRAS, 2002, 332, 49
Stetson P. B., 1994, PASP, 106, 250
Taam R. E., Bodenheimer P., 1989, ApJ, 337, 849
Walker A. R., 1999, AJ, 118, 432
Yanny B., Guhathakurta P., Bahcall J. N., Schneider D. P., 1994, AJ, 107, 1745

This paper has been typeset from a TEX/LATEX file prepared by the author.